Electrochimica Acta 280 (2018) 197–205

Contents lists available at ScienceDirect

Electrochimica Acta

journal homepage: www.elsevier.com/locate/electacta

The methanol and CO electro-oxidation onto Pt_{pc}/Co/Pt metallic multilayer nanostructured electrodes: An experimental and theoretical approach

C.D. Silva [a], L.H. Morais [b], R. Gonçalves [a], R. Matos [a, c], G.L.C. Souza [b], R.G. Freitas [a, b], E.C. Pereira [a, *]

[a] LIEC, Laboratório Interdisciplinar de Eletroquímica e Cerâmica, Departamento de Química, Universidade Federal de São Carlos, São Carlos, SP, Brazil
[b] LCM, Laboratório Computacional de Materiais, Departamento de Química, Universidade Federal do Mato Grosso, Cuiabá, MT, Brazil
[c] Departamento de Química, Universidade Estadual de Londrina, Londrina, PR, Brazil

ARTICLE INFO

Article history:
Received 30 January 2018
Received in revised form
18 April 2018
Accepted 20 May 2018
Available online 21 May 2018

Keywords:
Nanostructured electrodes
Methanol electro-oxidation
Metallic multilayer
Materials modelling

ABSTRACT

We developed Pt_{pc}/Co/Pt nanostructured metallic multilayers (MM) electrodes for methanol and carbon monoxide electro-oxidation. This material uses as an intermediate layer a non-noble metal (cobalt), which is a low cost material. Cyclic voltammetry was used to characterize the electrode electrochemical behaviour for methanol and carbon monoxide. In addition, electrochemical impedance spectroscopy (EIS) was used to study the methanol oxidation on these multilayers. An increase in the peak current density of about 35% for $Pt_{pc}/Co_{10}/Pt_5$ nanostructured metallic multilayer compared to Pt_{pc} electrode was observed for methanol oxidation reaction (MOR). Carbon monoxide electro-oxidation showed large current density for all multilayers electrodes and the onset potentials for this reaction was displaced toward more negative potentials, which indicates weaker adsorption energy for CO over the surface of the materials compared to Pt_{pc}. EIS data indicated a lower charge transfer resistance (R_{ct}) for $Pt_{pc}/Co_{10}/Pt_5$ MM nanostructured during the methanol electro-oxidation, that indicates higher electrocatalytic activity for this electrode compared to Pt_{pc}. Computational modelling results indicate that the presence of a Co-underlayer for Pt/Co/Pt (111) nanostructured system decrease the center of *d*-band and, consequently, increase the catalytic activity compared to Pt (111) system.

1. Introduction

Several selective catalysts and new fuels have been proposed in recent years to increase fuel cell efficiency [1,2]. Among the fuels, methanol is a promising one for direct oxidation fuel cells, DOFC, and many catalysts have been synthesized by modifying their structural properties to improve their catalytic activity.

In the DOFC, the modification of the platinum-based electrodes, as, for example, alloying it with different elements [3–5] or using different synthesis methods to prepare Pt thin film electrodes has been proposed to reduce the problems associated with the poisoning of the catalytic surface due to adsorption of CO.

A different approach is to build heterostructures using multi-metallic layers of Pt with a second element that have been used by our group in the last years [6–10] to study the electro-oxidation of small organic molecules.

The deposition of metallic multilayers, each one few nanometers thick, has attracted scientific and technological interest, once these layers present unexpected magnetic properties [11,12]. The structural and electronic changes presented by metallic multilayers structures have also attracted scientific interest. Kolb et al. demonstrated that monolayers of a metal deposited on different metal substrates may be subject to the strain effect, causing changes in the d-band center and in the stability of adsorbed CO [12]. Nørskov et al. proposed that the effect due to variations in the number of layers of a thin film of metals deposited in another metal can be described in terms of the d-band model [13]. The relationship between adsorption energies and catalytic activity has been established through models to study surface processes using density functional theory (DFT) calculations [14–19]. Nørskov et al. studied the modification of the chemical and electronic properties of Pt (111) surfaces by subsurface 3d transition metal using DFT,

* Corresponding author.
E-mail address: ernesto@ufscar.br (E.C. Pereira).

https://doi.org/10.1016/j.electacta.2018.05.127
0013-4686/

showing that the adsorption properties of molecules on transition metal surfaces can be adjusted by changes in the band surface structure d by strain induced shifts or the ligand effect [20]. Mavrikakis et al. studied competitive paths for the decomposition of methanol in Pt(111) using DFT calculations, which suggested that an energetically viable path is the decomposition of methanol through CH_2OH and formaldehyde or HCOH intermediates and another route is OH scission to CH_3O, followed by sequential dehydrogenation for CO [21].

The heterostructures employing cobalt in their compositions have become interesting because Co adlayers on Pt surfaces exhibit a strong magnetic anisotropy useful in the fabrication of magnetic storage devices [22–25]. Moreover, it has characteristics such as high hardness, thermal stability, corrosion resistance and low cost, that allow its application in the production of alloys and in the microelectronics industry.

Most of these Co overlayers have been prepared employing molecular beam evaporation techniques [26,27], and although it has been reported electrodeposition of cobalt [28,29], few studies have considered this last procedure as route to obtain Co overlayers onto Pt_{pc} [30–32]. Electrodeposition has important advantages, such as price and simplicity, but it requires the knowledge of nucleation and growth processes to synthesize deposits with reproducible properties.

Some alloys and core-shell materials have been studied for methanol electro-oxidation. Kwon et al. synthesized Pt-Co/CNT with Co-content 46.6 at % with high Pt contents, showing 2–3 fold improvement in mass and specific current in methanol electrooxidation compared to commercial Pt/C (60 wt%) [33]. Coville et al. prepared bimetallic nanoparticles of Pt bonding with Co, using the conventional heat-treatment method and microwave irradiation [34]. This study indicated an increase in the electrocatalytic activity with the addition of Co compared to monometallic Pt [34]. Etman et al. studied the synthesis of Pt-Co nanoparticles on MWCNT for methanol electro-oxidation in acidic solution, observing an increase in the peak current density of about 300%, and the peak potential shifted 80 mV towards more negative potential values for Pt-Co/MWCNT compared to Pt/MWCNT [35]. Valiollahi et al. synthesized Pt-Co/G/GCE, which showed higher peak current density and the onset potential more negative than Pt bulk and Pt-Co/GCE, indicating higher catalytic activity of this material for methanol electro-oxidation [36].

From a different point of view, our group have published a series of papers investigating the oxidation of small organic molecules using metallic multilayers [7–10,37]. In the last published paper, we have studied the methanol electro-oxidation on $Pt_{pc}/Rh_{2.0}/Pt_{1.0}$ metallic multilayer using electrodeposition technique and an enhancement on peak current density of 90% for this electrode compared to Pt_{pc} was observed during an oscillatory regime [37]. The authors suggested, using numerical simulation, that this increase in the electrocatalytic activity of this electrode could be related to the inhibition of adsorption of carbon monoxide on the surface of the metallic multilayer during the oxidation, indicating the direct pathway of reaction leading to the final production of carbon dioxide. Therefore, in that work [37], the authors proposed that carbon monoxide could act as a poisoning species instead of a reaction intermediate during the electro-oxidation of methanol.

Considering these aspects, this work aims at the preparation of $Pt_{pc}/Co/Pt$, a metallic multilayers nanostructured electrode that uses a non-noble metal (cobalt) as the intermediate layer, with different number of monolayers of the intermediate layer and the outer layer ($Pt_{pc}/Co_{ML}/Pt_{ML}$) for the methanol and CO electro-oxidation. The surface of the electrodes was characterized by atomic force microscopy (AFM) and the electrocatalytic activity for methanol and CO electro-oxidation were measured by cyclic voltammetry (CV). Moreover, electrochemical impedance spectroscopy (EIS) was used to characterize the methanol oxidation in the electrodes.

2. Experimental

A polycrystalline Pt_{pc}, area = 0.3 cm^2, was utilized as substrate to prepare the metallic multilayer electrode. The Pt_{pc} electrode was polished with diamond paste (Arotec) down to 1.0 μm and washed with acetone and purified water (Milli- Q system) several times.

The cobalt layer was deposited onto this substrate using a 10^{-5} mol L^{-1} $CoSO_4$ (Mallinckrodt) solution in 0.1 mol L^{-1} Na_2SO_4 (Synth) and 0.01 mol L^{-1} H_3BO_3 (Merck). The deposition potential was −0.65 V (vs. a reversible hydrogen electrode, RHE) for 10 s or 20 s leading to a charge equivalent to 5 or 10 Co monolayers (MLs), respectively. The platinum layer was electrodeposited over the Co layer from a 5.0×10^{-4} mol L^{-1} H_2PtCl_6 (Sigma-Aldrich) in 0.1 mol L^{-1} $HClO_4$ (Sigma-Aldrich, 70%) at 0.05 V (vs. RHE) for 100 s or 200 s to obtain 5 and 10 ML, respectively. The electrode $Pt_{pc}/Co_{ML}/Pt_{ML}$ was produced by this procedure. As auxiliary and reference electrodes, two Pt sheets (a = 1 cm^2) and a reversible hydrogen electrode in the same solution, RHE, were used, respectively.

Before the experiments, the $Pt_{pc}/Co_{ML}/Pt_{ML}$ electrode was electrochemically cleaned by repetitive potential cycling between 0.05 and 1.55 V (vs. a reversible hydrogen electrode, RHE) in the supporting electrolyte 0.1 mol L^{-1} $HClO_4$ (Sigma-Aldrich, 70%).

Prior to the experiments, the solutions were sparged with N_2 for 15 min. Voltammetric curves for methanol oxidation (one cycle) were measured in 0.1 mol L^{-1} $HClO_4$ (Sigma-Aldrich, 70%) solution containing 0.5 mol L^{-1} methanol (Sigma-Aldrich). CO (99.25%, White Martins) stripping measurements were performed to compare the catalytical properties of Pt_{pc} and MM electrodes. In these last experiments, CO was adsorbed on the working electrode by bubbling CO gas in 0.1 mol L^{-1} $HClO_4$ (Sigma-Aldrich, 70%) solution for 12 min prior to the experiments. Then, the solution dissolved CO was removed from the solution by bubbling nitrogen (99.0% min., Liquid Nitrogen) gas for 12 min maintaining the applied potential at 0.05 V. Finally, the applied potential to the working electrode is swept from 0.05 V up to 1.55 V at $v = 50$ mV s^{-1}.

Electrochemical impedance spectroscopy (EIS) was measured in a solution of 0.1 mol L^{-1} $HClO_4$ with 0.5 mol L^{-1} of methanol using an excitation AC signal of 5 mV_{rms} in the frequency range from 10 kHz to 10 mHz using the Autolab PGSTAT 30 coupled to the frequency response analyser, FRA, module. The impedance data analysis was performed with EIS Spectrum Analyser software package [38], where the spectra were fitted by means of non-linear least-squares procedure.

Finally, the electrode surfaces were characterized by atomic force microscopy (AFM) using SPM 5500-Agilent equipment in contact mode.

2.1. Computational methods

The density functional theory [39,40] calculations were performed using Quantum-ESPRESSO package [41]. The electron-ion interaction was described by Ultra-soft pseudopotentials (US-PP) with scalar relativistic correction generated by Rappe-Rabe-Kaxiras-Joannopoulos method (RRKJUS) [42]. The generalized gradient approximation (GGA) for the exchange-correlation (*xc*) density functional Perdew-Burke-Ernzerhof (PBE) [43] was used in all calculations reported herein. The chosen energy cutoff was 30 Ry and the threshold for self-consistency was 10^{-6} eV. Slab atoms were held in their bulk truncated positions and relaxation of

adlayer was allowed in all directions until all force components acting on adatoms were below 0.05 eV $Å^{-1}$.

The (2×2) unit cell representing system is four layers thick ensemble of closed-packed Pt (100) metal. The Pt_{MM} system consist of 4 Pt layer and $Pt/Co_{ML}/Pt_{ML}$ consist of 3 Pt layers and 1 Co monolayer. For both systems, the two uppermost metal layers were allowed to relax and two others kept freeze. Approximately five layers of vacuum (15 Å) thick were used to separate the periodic images along the *z*-direction of the supercell. The Brillouin zone is sampled with a uniform 7×7 x 1 *k*-points grid [44]. Lattice constants (a_{Pt}) were set to the experimental values [45]. Convergence of the total energy and with respect to the cut off energies and *k*-points set was used as the criteria of the correctness of the procedure.

The projected density of states (PDOS) in the atoms and orbital was built for the analysis of the corresponding electronic structure. The XCrysDen program [46] was used to draw the surfaces.

3. Results and discussion

Typical AFM images of Pt_{pc}, Pt_{pc}/Co_{10} and $Pt_{pc}/Co_{10}/Pt_5$ surfaces are presented in Fig. 1, where it is possible to observe terraces, steps and kinks. The scratches observed on the surfaces are in agreement with Pt_{pc} AFM images obtained by Udisti et al. [47], and are related to the polishing cleaning procedure. It is well-know that metal deposition starts at surface defects, e.g. steps and kinks sites being the most favourable nucleation centers [48] and the deposit morphology is strongly affected by the density and distribution of such defects, especially during the initial stages of growth [48].

For a more detailed study about the nucleation-and-growth related to Co and Pt overlayers onto Pt_{pc} substrate, the roughness mean square (RMS) was obtained at three different regions on the electrode surface. It is not observed any significant difference among the electrodes as shown in Table 1. These values are in agreement with those described on the literature. The morphology presented in Fig. 1 indicate a surface with granular morphology overall. Georgescu et al. studied the electrodeposition of Co/Pt thin films with several Co layer thickness [30]. The authors also observed a granular morphology to their metallic multilayer, and the higher RMS values obtained (16.3–44.0 nm) could be related to different substrate and electrochemical technique applied [30].

As discussed above, the RMS values obtained for Pt_{pc} and $Pt_{pc}/Co_{10}/Pt_5$ were similar. Therefore, any difference in the electrochemical behaviour of MM compared to Pt_{pc} cannot be related to surface area changes.

The cyclic voltammogram of Pt_{pc}, $Pt_{pc}/Co_{10}/Pt_5$ and $Pt_{pc}/Co_5/Pt_{10}$ MM electrodes are presented in Fig. 2.

In order to obtain a reproducible surface, prior to the experiments, all the electrodes were cycled between 0.05 and 1.55 V at 1 V s^{-1} for 900 cycles. A typical polycrystalline Pt profile reported on the literature [49] can be observed for the MM electrodes here prepared. The electrochemical processes observed for the Pt_{pc} and MM nanostructured electrodes can be associated to surface process and approximately potential regions, described below: *i)* hydrogen adsorption and desorption between 0.05 and 0.4 V, *ii)* double layer region between 0.4 and 0.8 V and *iii)* formation and reduction of PtO, between 0.8 and 1.55 V and 1.55 V and 0.4 V, respectively [49]. Then, the electrode surface area was calculated using the procedure well established in the literature [50]. In the procedure, the charge under the voltammetric peaks for hydrogen adsorption or desorption, corrected for the capacitive component, is assumed to correspond to adsorption of one hydrogen atom on each metal atom of the surface [50]. In the case of Pt_{pc}, the value is 210 μC cm^{-2}. The values of the calculated electrochemically active surface areas for $Pt_{pc}/Co_{10}/Pt_5$ and $Pt_{pc}/Co_5/Pt_{10}$ are the same as the Pt_{pc}

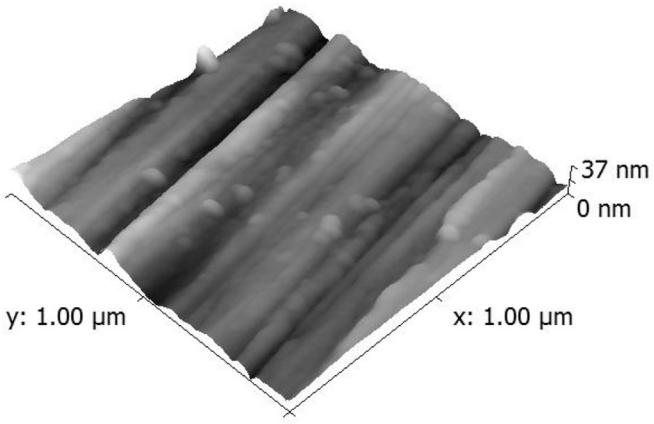

a

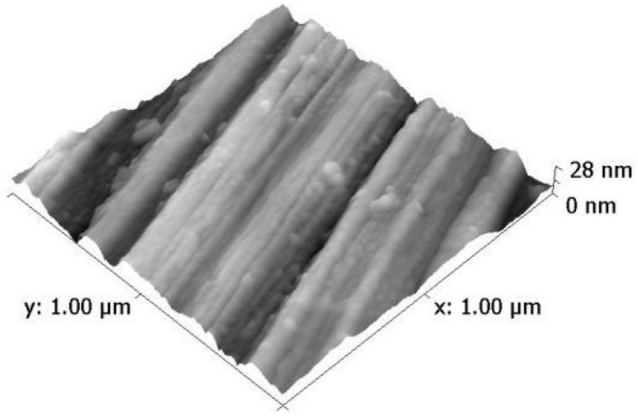

b

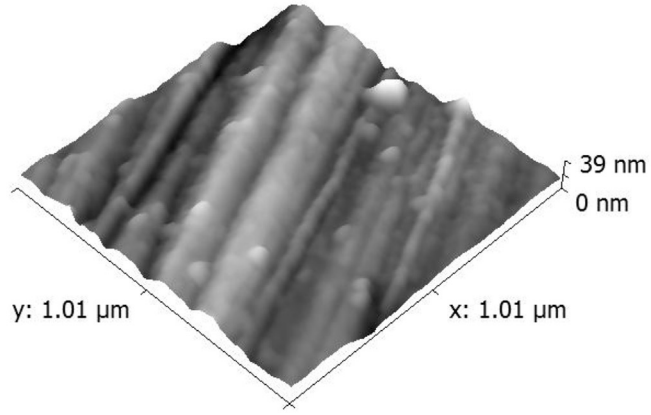

c

Fig. 1. 3D AFM images (1 μm × 1 μm) for: a) Pt_{pc}, b) Pt_{pc}/Co_{10} and c) $Pt_{pc}/Co_{10}/Pt_5$.

Table 1
Roughness medium square obtained at Pt_{pc}, Pt_{pc}/Co_{10} and $Pt_{pc}/Co_{10}/Pt_5$ using AFM.

Sample	RMS (Pt_{pc})/nm	RMS (Pt_{pc}/Co_{10})/nm	RMS ($Pt_{pc}/Co_{10}/Pt_5$)/nm
1	4.92	5.00	5.39
2	4.90	4.44	6.60
3	5.31	3.32	5.70
RMS	5.04 ± 0.2[a]	4.25 ± 0.8[a]	5.90 ± 0.6[a]

[a] Considering 95% confidence level *t*-test.

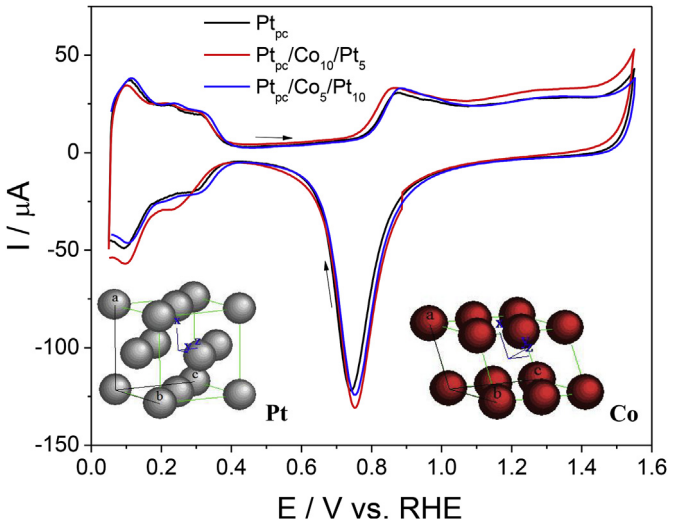

Fig. 2. Cyclic voltammograms for Pt_{pc}, $Pt_{pc}/Co_{10}/Pt_5$ and $Pt_{pc}/Co_5/Pt_{10}$ MM nanostructured electrodes in 0.1 mol L^{-1} $HClO_4$. Inset: Pt and Co crystalline structure. $\nu = 50$ mV s^{-1} and T = 25 °C.

(0.72 cm^2).

As can be observed in Fig. 2, the voltammetric profile of Pt_{pc} is completely recovered when MM nanostructured electrode is formed by the deposition of a Pt topmost surface over the Co underlying. It is macroscopic evidence that the electrode surface is now composed by Pt atoms. Moreover, there are no anodic currents which can be related to the oxidation/dissolution of Co in the voltammograms of Pt_{pc}/Co/Pt MM, demonstrating that Co is covered by the Pt layers. Also, there is no change in charge related to the H desorption process, and the active electrochemical area is the same for the $Pt_{pc}/Co_{10}/Pt_5$ and $Pt_{pc}/Co_5/Pt_{10}$ MM nanostructure (0.72 cm^2) in comparison to Pt_{pc} electrodes (0.72 cm^2). Jahns et al. studied up to about 6 monolayer of Co deposition on Pt(111) using molecular beam epitaxy [51]. The authors observed that Co grows as islands, in incoherent epitaxy with the Pt substrate distributed in face-centered cubic and hexagonal close package structures. Moreover, the authors observed that this deposition method induces surface segregation on the substrate Pt atoms, thereby generating a Pt-enriched topmost surface [51]. It could be observed using electrochemical *in situ* FTIR, whereas a new CO_{ads} band gives rise due to Pt-CO and Co-CO adsorption. Sugawara et al. also studied the deposition of Co and Pt onto Pt(111) single crystal using molecular beam epitaxy, leading to $Pt_{0.6nm}/Co_{0.3\,nm}/Pt(111)$ multilayer electrodes [52]. The authors observed that the epitaxial Co layer on the Pt(111) was unstable in the electrochemical environment [52]. Also, the voltammograms are pretty different before and after the linear sweep voltammograms related to the oxygen reduction reaction. It indicates that the outmost surface was reconstructed.

Adzic et al. observed the same Pt profile for Pt/C and Pt_{ML}/Pd@Co/C in acidic media as reported herein [53]. However, the authors observed different intensities on the process related to the hydrogen adsorption/desorption. Also, the authors observed that the beginning of Pt monolayer oxidation and the oxide-reduction peak shifted 70 and 60 mV to more anodic potentials respectively compared to Pt/C [53]. Therefore, it indicates that Pt oxides are less suitable to occur on a Pt monolayer than on pure Pt. The authors also observed this delayed on a Pt monolayer on the Co@Au/C surface using XANES [54].

The electronic properties of a Pt outmost surface can be significantly modified by the formation of an artificial superlattice. Consequently, it is possible to tuning the catalytic activity of MM nanostructured electrodes. Pt and Co have different crystallography parameter, and its unit cell were simulated here using the computational package Carine Crystallography 3.1 [55] using appropriated crystallography information files [56]. As observed on Fig. 2-inset, Pt is face-centered cubic and its unit cell volume is 62 $Å^3$. On the other side, cobalt is hexagonal-close packing and its unit cell volume is 22 $Å^3$. Analysing the large difference between Pt and Co unit cell volume, a compressive strain is expected due to the difference in the lattice constant comparing topmost Pt surface and Co underlying. The consequences of this change in the electronic parameters is, in such way, the change of some electrocatalytic processes and a tuning the electrocatalytic activity, which will be discussed below.

The CO stripping voltammogram is presented on Fig. 3 for Pt_{pc}/Co/Pt MM nanostructure and Pt_{pc} electrodes and it is in agreement with literature [57]. As observed, the current values associated to the H desorption region is complete suppressed. Evidence of the CO_{ads} saturation coverage was the complete blocking monolayer. Fig. 3 shows that two different regions can be distinguished for both surfaces: i) the so-called pre-ignition potential region (E < 0.55 V) and ii) the potential region where sharp stripping peaks are observed on the cyclic voltammogram (E > 0.55 V) [57]. Moreover, there is a distinct broad peak at ca 0.75 V before the main sharp peak of CO stripping for Pt_{pc}. This type of behaviour can be related to the mobility of the forms of CO, as linear, bridge and threefold on the surface of the electrode [58,59]. Analysing Fig. 3 it is possible to observe that the sharp stripping peak was shifted 130 and 68 mV towards more negative potential values for $Pt_{pc}/Co_{10}/Pt_5$ and $Pt_{pc}/Co_5/Pt_{10}$ MM nanostructured compared to Pt_{pc}, respectively. One possible explanation is an improve in the electrocatalytic activity for MM nanostructured surfaces compared to Pt_{pc} electrodes.

Zhang et al. found similar results studying Pt and PtCo catalysts dispersed on polypyrrole-multiwall carbon nanotube (PPy-MWCNT) matrix for methanol electro-oxidation [60]. The authors also observed that the sharp CO stripping peak shifted towards negative potential for PtCo/PPy-MWCNT compared to Pt/PPy-MWCNT and Pt/C [58]. According to Watanabe et al. the reason for improvement of CO-tolerance is that electronic structures of Pt-Co alloys are apparently different from that of Pt [61], which is applicable in the MM system. The authors observed using XPS, that Pt $4f_{7/2}$ energy bonding in Pt-Co alloys is lower than that in pure Pt,

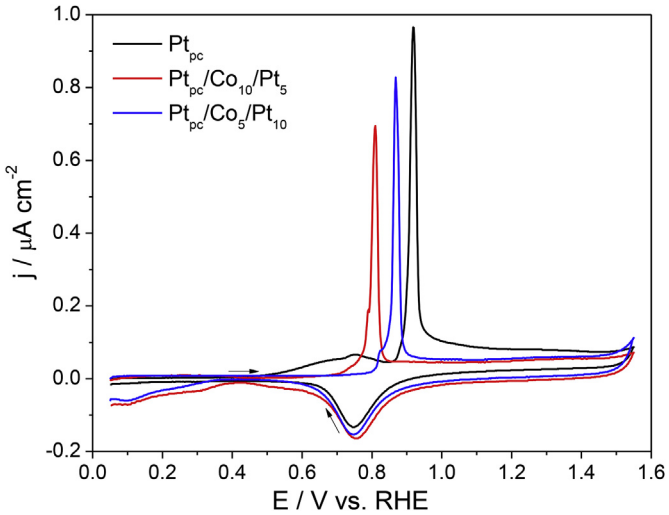

Fig. 3. CO stripping voltammogram on the a) Pt_{pc}, b) $Pt_{pc}/Co_{10}/Pt_5$ and c) $Pt_{pc}/Co_5/Pt_{10}$ MM nanostructured electrodes in 0.1 mol L^{-1} $HClO_4$. $\nu = 50$ mV s^{-1} and T = 25 °C.

which benefits the desorption of CO at low potential [59]. Medlin et al. studied the Pt/Co/Pt(111) surfaces *d*-band center distribution near the Fermi level using theoretical methods (*DFT*) comparing to Pt(111) [62]. According to the authors, Pt/Co/Pt(111) could exhibit a compressive structure, once that its center of *d*-band is shifted towards more negative values and the density of occupied states near the Fermi level is lower than Pt(111) surface [60]. Finally, in a more realistic model surfaces, Sugawara et al. studied CO electro-oxidation over $Pt_{0.3nm}/Co_{0.3\,nm}/Pt(111)$ multilayer electrode compared to $Co_{0.3\,nm}/Pt(111)$ surface using electrochemical *in situ* FTIR [52]. The authors observed that the C-O stretch frequencies of adsorbed CO depend strongly on the structure and composition of the topmost part of the surface. According to the authors, the center of linearly-bonded CO band observed for $Pt_{0.3nm}/Co_{0.3\,nm}/Pt(111)$ multilayer electrode is shifted towards lower wavenumber compared to $Co_{0.3\,nm}/Pt(111)$ surface [52]. It suggest that the CO_L is tight strength binding on $Co_{0.3\,nm}/Pt(111)$ surface than on $Pt_{0.3nm}/Co_{0.3\,nm}/Pt(111)$ multilayer electrode, which results in a highest electrocatalytic activity for multilayer electrodes. These results found in the literature are quite close that were found in the MM, although the present work got such results with a modified polycrystalline platinum electrode, which is a great vantage in terms of ease of manufacturing.

Linear voltammograms of $Pt_{pc}/Co/Pt$ metallic multilayer nanostructured and Pt_{pc} electrodes in the presence of methanol are illustrated in Fig. 4.

Methanol electro-oxidation at polycrystalline Pt presents the well-know oxidation profile [63,64] characterized by an oxidation peak at 0.86 V during the anodic sweep. This peak in the linear voltammogram appears at a potential where surface-bonded OH is formed on Pt, and these species have an important role in methanol electro-oxidation. The first process is attributed to oxidative removal of adsorbed/dehydrogenated methanol fragments (e.g. CO_{ads}) by oxygen-containing species PtOH [65,66]. During this process, CO_{ads}, CO_2, HCOOH, HCOH and $HCOOCH_3$ are formed and CO molecules reabsorb, poisoning the surface [61,62]. For higher anodic potentials, it is known that, for primary alcohols, the main species produced are HCOH, CO_2 and HCOOH [63,64]. It is possible to observe an enhancement on peak current density of about 35% for $Pt_{pc}/Co_{10}/Pt_5$ nanostructured metallic multilayer compared to Pt_{pc} electrode and the peak potential was shifted 100 mV towards more negative potential values for $Pt_{pc}/Co_{10}/Pt_5$ compared to Pt_{pc}. It can be indicated higher catalytic activity for $Pt_{pc}/Co_{10}/Pt_5$ MM nanostructured surfaces compared to Pt_{pc} electrodes.

The higher complexity and several dehydrogenation steps evolving in the methanol electro-oxidation compared to CO probe molecule, results in a decreasing of about 58% in the peak current density for $Pt_{pc}/Co_5/Pt_{10}$ nanostructured metallic multilayer surface. The peak potential was displaced approximately 20 mV towards more positive potential values for $Pt_{pc}/Co_5/Pt_{10}$ compared to Pt_{pc}, which can be indicated lower electrocatalytic activity compared to Pt_{pc}.

Etman et al. studied the synthesis of Pt-Co nanoparticles on MWCNT for methanol electro-oxidation in acidic solution [67]. The authors observed an increase in the peak current density of about 300%, and the peak potential shifted 80 mV towards more negative potential values for Pt-Co/MWCNT compared to Pt/MWCNT [65]. According to them, this increasing in the electrocatalytic activity can be explained by the fact that alloying Co together with Pt lowers the electronic binding energy to enhance the C-H cleavage reaction at lower potential values [65]. Additionally, CO oxidation reaction can be facilitated by the presence of cobalt oxides, which absorbs OH species [68]. Analysing the methanol electro-oxidation over $Pt_{pc}/Co/Pt$ MM electrodes, the results could be explained by the electronic interaction between the platinum exposed surface and the cobalt intermediate, which can facilitate the CO oxidation in smaller potentials resulting in the improvement of the electrocatalytic activity for $Pt_{pc}/Co_{10}/Pt_5$ nanostructured metallic multilayer surface in the methanol oxidation.

Electrochemical impedance spectroscopy (EIS) was used in order to determine the charge transfer resistance during the methanol electro-oxidation process at Pt_{pc}, $Pt_{pc}/Co_{10}/Pt_5$ and $Pt_{pc}/Co_5/Pt_{10}$ MM nanostructured electrodes. Fig. 5 shows the Nyquist spectra obtained in a solution of 0.5 mol L^{-1} methanol in 0.1 mol L^{-1} $HClO_4$ at 0.8 V and the equivalent circuits used to fit these data.

The Nyquist plot (Fig. 5a) shows a typical spectrum for Pt_{pc}, a compressed semicircle as response to a non-ideal capacitance behaviour. In the other hand for the MM samples the semicircle occurs just until 0.5 Hz for $Pt_{pc}/Co_{10}/Pt_5$ electrode and until 1.25 Hz for $Pt_{pc}/Co_5/Pt_{10}$ electrode; below these frequencies they present an

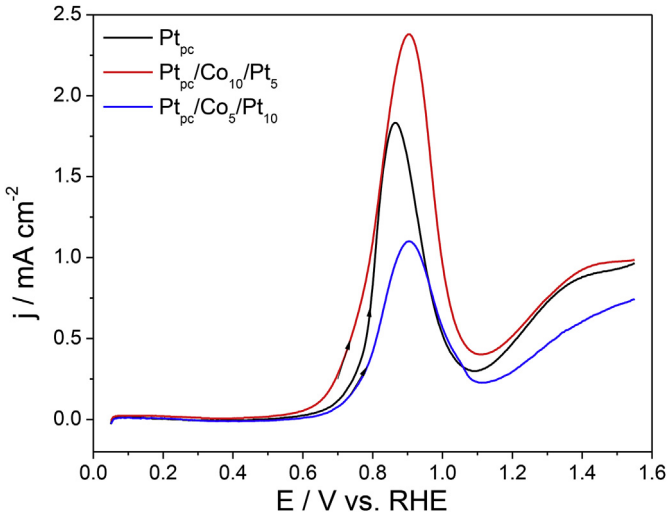

Fig. 4. Linear voltammograms obtained for the electro-oxidation of 0.5 mol L^{-1} methanol in 0.1 mol L^{-1} $HClO_4$, $\nu = 50$ mV s^{-1} a) Pt_{pc}, b) $Pt_{pc}/Co_{10}/Pt_5$ and c) $Pt_{pc}/Co_5/Pt_{10}$ MM nanostructures electrodes.

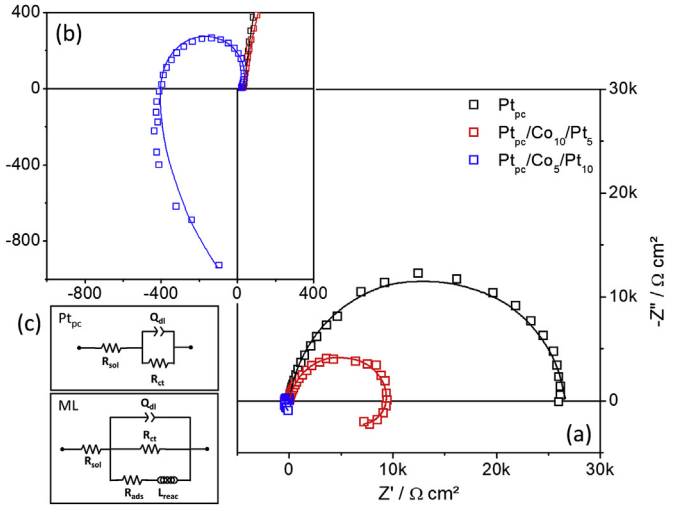

Fig. 5. a) Nyquist plots of EIS for methanol electrooxidation electrochemically polarized at 0.8 V on the Pt_{pc}, $Pt_{pc}/Co_{10}/Pt_5$ and $Pt_{pc}/Co_5/Pt_{10}$ MM nanostructures electrodes, b) Inset od Nyquist zoom of $Pt_{pc}/Co_5/Pt_{10}$ data. T = 25 °C. c) Equivalent circuit used to fitting the spectra data.

inductive response. This inductive behaviour had been explained by Muller et al. [69] using the kinetic theory derived by Harrington and Conway [70] for reaction involving intermediate adsorbates:

$$CH_3OH \rightarrow CO_{ads} \rightarrow CO_2 \quad (1)$$

Moreover, it is possible to observe that for $Pt_{pc}/Co_5/Pt_{10}$ (Fig. 5b) the R_{ct} is negative, which could be related to passivation of the electrode surface. Melnik and Palmore indicated that the passivation of the Pt electrode during methanol electro-oxidation is due to the reversible formation of oxide species [68]. The formation of a system with bifurcation and oscillatory behaviour can also be analysed in light of negative R_{ct} [71]. Although a systematic explanation about the Co and Pt deposition mechanism (Frank-van der Merve [72], Volmer-Weber [73] and Stranski-Krastanov [73]) is undertaken, the Co-Pt interdiffusion could also be considered as a reason for R_{ct} negative values. Shen et al. studied the Co monolayers deposition onto Pt(111) using sputtering [73]. According to the authors, the growth of Co monolayer onto Pt(111) belongs to Stranski-Krastanov mode, and the activation energy and diffusion coefficient for the Co-Pt alloy formation were 0.9 eV and 6.6×10^{-11} cm^2 s^{-1} respectively [74]. Nastasi et al. studied the Co/Pt multilayers deposited onto Pt-coated(001) MgO(0001) using e-beam evaporation [74]. The authors observed that the activation energy for interdiffusion depends on crystal orientation, *e.g.*, 1.1 eV and 0.8 eV for (001) and (111) Co/Pt multilayers [75]. This Co-Pt interdiffusion could be explained in light of an internal coherency strains that increase the equilibrium vacancy concentration and enhance atom mobility (normal to the film plane) in the Co layers. Alternatively, the presence of low resistance diffusion paths, such as dislocations, in the monolayers could be a different explanation for this result.

Fig. 5c shows the equivalent circuits used to fit the impedance data. In the first plane was assumed that mass transport limitation does not occurs. Thus, in such way, in the lower frequency part of the data is also regarding to electrode surface process. The Pt_{pc} spectrum was fitted using a modified Randles model were the Q_{dl} is used to explain the *pseudo* capacitive behaviour at the electrode surface; R_{ct} is the charge-transfer resistance associated with methanol electro-oxidation and the solution resistance is represented as R_{sol}. For the MM, besides the same circuit elements of the Pt_{pc} electrode, is used the R_{ads} and L_{ads} in series with other, which are associated with the adsorption process of intermediates formed during methanol electro-oxidation, both in parallel to the R_{ct} 74. The values of the circuit elements, as well as the χ^2 for each adjustment, which confirms the good fit of the models used, are presented in Table 2.

The charge transfer resistance obtained from simulation of the impedance spectra were 26.4 k^O cm^2 and 10.0 k^O cm^2 for Pt_{pc} and $Pt_{pc}/Co_{10}/Pt_5$ MM nanostructured electrodes respectively. Therefore, providing a faster charge transfer kinetics rates during methanol electro-oxidation on $Pt_{pc}/Co_{10}/Pt_5$ MM nanostructured compared to Pt_{pc} electrodes and a higher electrocatalytic activity.

Fig. 6 presents the Bode plots where is possible to see important information associated to the frequency modulation. Thus, in Fig. 6a is observable for the MM samples there is a small inflection that is associated to the appearance of the inductive part. Besides, as previously mentioned, such behaviour is not observed for the Pt_{pc}, which presents an increasing value of |Z| until a plateau at its maximum value. To that end, in Fig. 6b, also for the sample Pt_{pc}, the phase angle signal does not change, which is indicative of the quadrant change in impedance. This fact is observed in the Pt/Co/Pt samples, in especial for $Pt/Co_5/Pt_{10}$ that presents two quadrant changes.

The inductive behaviour could be rationalized by postulating slowness of CO_{ads} coverage relaxation. The CO_{ads} coverage decreases with increasing potential [76], but it takes some time after a potential perturbation before the new steady-state coverage is established and the corresponding current flows. This phase-delay leads to the observed inductive behaviour on the spectra (Fig. 6b). While Pt_{pc} did not present an inductive part, $Pt_{pc}/Co_5/Pt10$ and $Pt_{pc}/Co_{10}/Pt_5$ MM nanostructured electrodes presented 24.5 and 188 kH, respectively. Thus, the slowness of CO_{ads}-coverage relaxation is larger on $Pt_{pc}/Co_5/Pt10$ compared to $Pt_{pc}/Co_{10}/Pt_5$, resulting in a higher electrocatalytic activity of the second one. Wang et al. studied PtRu/C and PtRu/C using Nd_2O_3 as dispersing agent for methanol electro-oxidation [77]. The authors also observed lower inductive values for electrodes with higher electrocatalytic activity for, i.e. PtRu/C using Nd_2O_3 electrodes [75]. Therefore, the inductive loop in methanol electro-oxidation indicates that the CO_{ads} coverage on Pt_{layer} surface decreases due to changes in the electronic properties and the decrease in CO_{ads} leads to an increase of

Table 2
Electrochemical area normalized values obtained of R_{sol}, Q_{dl}, n_{dl}, R_{ct}, R_{ads} and L_{reac} for the electrodes samples.

Circuit elements	Pt_{pc}	$Pt_{pc}/Co_{10}/Pt_5$	$Pt_{pc}/Co_5/Pt_{10}$
R_{sol}/kΩ cm^2	33.0	30.5	23.3
R_{ct}/kΩ cm^2	26.4	10.0	−0.370
Q_{dl}/μF s^{n-1} cm^{-2}	4.43	11.8	1.28
n_{dl}	0.925	0.901	0.795
R_{ads}/kΩ cm^2	–	8.86	0.329
L_{reac}/kH	–	25.5	188
χ^2	1.60×10^{-3}	7.37×10^{-4}	2.39×10^{-3}

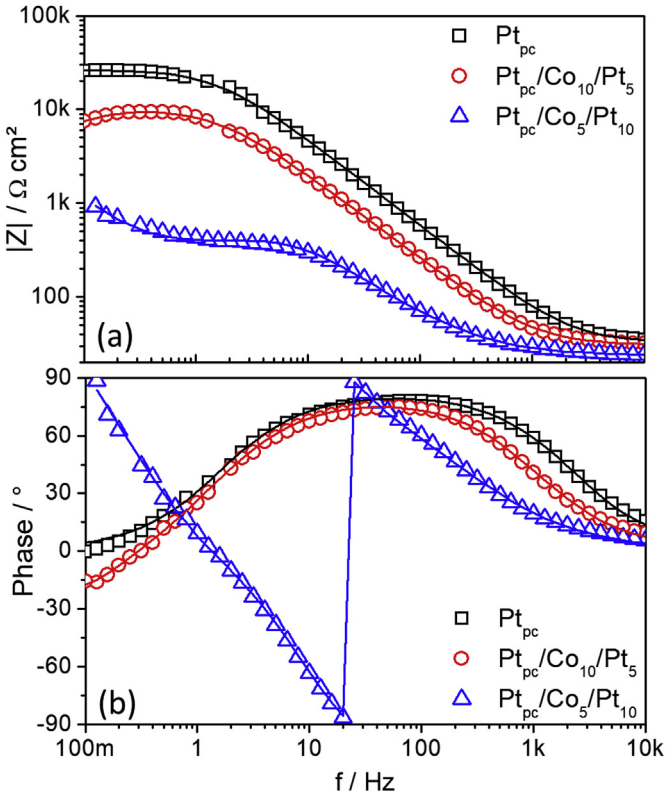

Fig. 6. a) Bode Modulus and b) Bode Phase plots of EIS for methanol electrooxidation electrochemically polarized at 0.8 V on the Pt_{pc}, $Pt_{pc}/Co_{10}/Pt_5$ and $Pt_{pc}/Co_5/Pt_{10}$ MM nanostructures electrodes. T = 25 °C.

Faradaic current. A reasonable explanation for this observation is that enough OH_{ads} groups on Pt_{layer} sites are formed, as can be observed on the earlier water activation (0.45 V) in Fig. 4 for Pt_{pc}/Co_{10}/Pt_5 MM nanostructured electrodes. The as-formed OH_{ads} groups are then used to oxidize CO_{ads} to decrease CO poisoning, generating more refreshed Pt_{layer} sites for methanol adsorption to enhance the Faradaic current. As observed above Pt_{pc}/Co_{10}/Pt_5 MM nanostructured electrodes presents higher electrocatalytic activity for CO and methanol oxidation compared to Pt_{pc} system.

Therefore, such cobalt intralayer is fundamental to tuning structural and electronic properties of multilayers. In order to probe the electronic effects of cobalt intralayer, a small theoretical ensemble based on Pt (100) and Pt/Co/Pt (100) were simulated, as presented in Fig. 7 a and b, respectively.

The platinum lattice constant obtained was $a_0 = 3.923$ Å for both for Pt (100) and Pt/Co/Pt (100) system, which is in agreement with experimental values $a_0 = 3.920$ Å obtained using Rietveld refinement [45]. However, the distance between layers were $d_{12} = 1.9615$ Å, $d_{23} = 1.9964$ Å, $d_{34} = 1.9811$ Å and $d_{12} = 1.9615$ Å, $d_{23} = 1.8420$ Å, $d_{34} = 1.8244$ Å for Pt (100) and Pt/Co/Pt (100) system. Therefore, it can be observed that the insertion of a foreign monolayer e.g. cobalt decrease the distance between interlayer spacings. Such decrease leads to tuning the electronic and catalytic effects of Pt-top most layer. Finally, as can be observed d_{12} were the same for Pt (100) and Pt/Co/Pt (100) system, once that 2-botom layer were kept freeze. Such decreasing along the interlayer spacing can be explained in spotlight of well-know Heide et al. model which explain how the surface atoms can be expected to relax [78]. This model predicts *i)* a small contraction for the first interlayer spacing; and *ii)* that the contraction is more pronounced for open surfaces that for closed-packed ones. According to Scheffler et al. [79] the physical basis of the model is the Smoluchowski smoothing of the electron charge density at the surface [80]. When a crystal is cut to form a surface, the electron rearrange in order to reduce the charge-density corrugation and by this way their kinetic energy. This leads to a motion of the electron left on top of the surface atom downward to the crystal resulting in an electrostatic attraction of the top layer ins toward the rest. To the best of our acknowledgment, this is the first report of interlayer spacings and its relation with electrocatalytic properties, once that platinum lattice parameter (a_0) observed were the same for Pt (100) and Pt/Co/Pt (100) system.

Two other effects are presented in Pt/Co/Pt (100) which can explain its higher electrocatalytic properties compared to Pt (100) system: i) a geometric effect arises due to a lattice strain introduces by the epitaxial replacement of Pt atoms by Co intra-monolayer and ii) electronic effect due to the bonding between Co-intralayer and Pt-host metal which necessarily has a different electronic configuration. The synergism of both effects acts in order to tuning the reactivity of Pt/Co/Pt (100) compared to Pt (100) system and can be studied using the energies of *d*-band centers (ε_d).

The shift of *d*-band center were calculated as the center of gravity of *d*-state's projected density of states (*d*-PDOS) of Pt atoms, as presented in Fig. 7c. The *d*-band center obtained for Pt (100) and Pt/Co/Pt (100) system were −2.491 eV and −2.799 eV, respectively. Therefore, the presence of Co-intralayer shift the *d*-band center 0.308 eV towards negative values. Chen et al. also studied the center of *d*-band for Pt (111) and obtained −2.44 eV [20], which

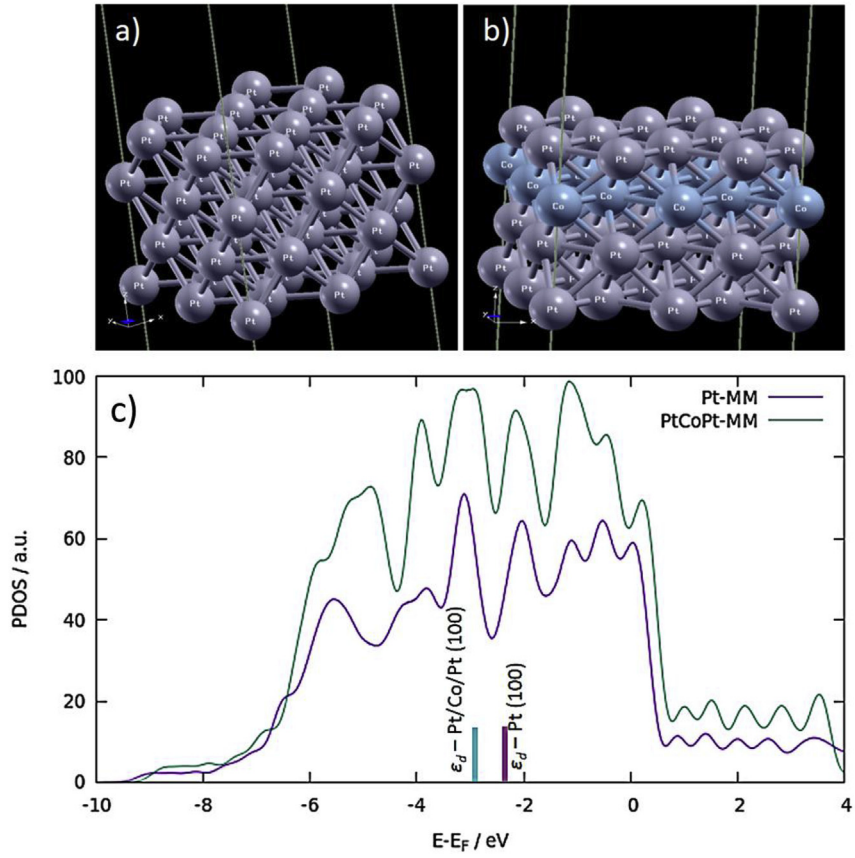

Fig. 7. Theoretical ensemble based on: a) Pt (100), b) Pt/Co/Pt (100) and c) the shift d-band center shift calculated as the gravity center of *d*-states projected density of states (*d*-PDOS) Pt atoms.

indicate that such data is in agreement with literature.

Once that *sp* bands of the metals are broad and structureless, the *d*-bands are narrow, and small changes in the environment (such as Co-intralayer) can change the *d* states and their interaction with adsorbate states significantly. Also, according to Chen et al. the interaction between adsorbates and transition metal surfaces involve the entire *d*-band [20]. The high lying *d*-band center (close to Fermi level) implies that antibonding states created by adsorption will lie above the Fermi level-thus they area empty states and lead o strong adsorption. Therefore, according to our simulation Pt (111) are more prone to exhibit strong adsorption with methanol and by-products than Pt/Co/Pt (111) system, which induces a higher electrocatalytic activity for nanostructured electrodes [6–10,37].

4. Conclusions

In this work, metallic multilayers nanostructured electrodes Pt_{pc}/Co/Pt, that uses a non-noble metal as an intermediate layer, was developed for the methanol and CO electro-oxidation. The electrode $Pt_{pc}/Co_{10}/Pt_5$ showed improve in catalytic activity with increases of 35% in peak current density and a displacement of the onset toward more negative potentials. For the CO oxidation, a displacement of 130 and 68 mV towards more negative potential values for $Pt_{pc}/Co_{10}/Pt_5$ and $Pt_{pc}/Co_5/Pt_{10}$ MM nanostructured compared to Pt_{pc} was observed, which indicates weaker adsorption energy for CO over the surface of the materials compared to Pt_{pc}. The R_{ct} for $Pt_{pc}/Co_{10}/Pt_5$ MM nanostructured during the methanol electro-oxidation process was lower than Pt_{pc}, also indicating an improvement in the electrocatalytic activity for this electrode compared to Pt_{pc}, while the $Pt_{pc}/Co_5/Pt_{10}$ electrode presented a negative R_{ct}, which may be related to electrode passivation or to oscillatory processes. Thus, the use of metallic multilayers becomes promising in studies about the methanol electro-oxidation.

Computational modelling indicate a decreasing in the lattice spacing which affect the ligand/electronic effects and tuning the catalytic properties for Pt/Co/Pt (111) compared to Pt (111) system. Also, the insertion of a Co under-layer lead to a decreasing in the *d*-band center observed for Pt/Co/Pt (111) system and probably a weaker adsorption energy with methanol and by-products. Such synergism of effects lead to highest catalytic activity observed for Pt/Co/Pt (111) system. The theoretical effect of Pt (top-most layer) and Co (under-layer) thickness is not well understanding yet. Based on ensemble size, materials modelling concerning only few layers data are observed on the literature. Therefore, this paper spotlight the importance of the experimental and theoretical modelling of layers thickness (under and top) in order to tuning the catalytic effects.

Acknowledgments

The authors would like to thank the Brazilian Research Funding Institutions CNPq (427161/2016-9), CAPES, FAPEMAT (214599/2015) and FAPESP (2013/07296-2, 2010/05555-2 and 2009/16530-3) for financial support. We are also grateful to CENAPAD/SP (Proj650) for providing the computational time.

References

[1] B.Y. Xia, H.B. Wu, N. Li, Y. Yan, X.W. Lou, X. Wang, One-pot synthesis of Pt-Co alloy nanowire assemblies with tunable composition and enhanced electrocatalytic properties, Angew. Chem. Int. Ed. 54 (2015) 3797.
[2] E. Lee, S. Kim, J. Jang, H. Park, M.A. Matin, Y. Kim, Y. Kwon, Effects of particle proximity and composition of Pt–M (M= Mn, Fe, Co) nanoparticles on electrocatalysis in methanol oxidation reaction, J. Power Sources 294 (2015) 75.
[3] J.P.I. de Souza, S.L. Queiroz, K. Bergamaski, E.R. Gonzalez, F.C. Nart, Electro-oxidation of ethanol on Pt, Rh, and PtRh electrodes. A study using DEMS and in-situ FTIR techniques, J. Phys. Chem. B 106 (2002) 9825.
[4] J. Jiang, T. Aulich, High activity and durability of Pt catalyst toward methanol electrooxidation in intermediate temperature alkaline media, J. Power Sources 209 (2012) 189.
[5] R. Awasthi, R.N. Singh, Graphene-supported Pd–Ru nanoparticles with superior methanol electrooxidation activity, Carbon 51 (2013) 282.
[6] R.G. Freitas, E.C. Batista, M.P. Castro, R.T.S. Oliveira, M.C. Santos, E.C. Pereira, Ethanol electrooxidation on Bi submonolayers deposited on a Pt electrode, Eletrocatalysis 2 (2011) 224.
[7] R.G. Freitas, E.P. Antunes, E.C. Pereira, CO and methanol electrooxidation on Pt/Ir/Pt multilayers electrodes, Electrochim. Acta 54 (2009) 1999.
[8] R.G. Freitas, M.C. Santos, R.T.S. Oliveira, L.O.S. Bulhoes, E.C. Pereira, Methanol and ethanol electroxidation using Pt electrodes prepared by the polymeric precursor method, J. Power Sources 158 (2006) 164.
[9] R.G. Freitas, L.F. Marchesi, R.T.S. Oliveira, F.I. Mattos-Costa, E.C. Pereira, L.O.S. Bulhões, M.C. Santos, Methanol oxidation reaction on $Ti/RuO_{2(x)}Pt_{(1-x)}$ electrodes prepared by the polymeric precursor method, J. Power Sources 171 (2007) 373.
[10] R.G. Freitas, E.C. Pereira, P.A. Christensen, The selective oxidation of ethanol to CO2 at Ptpc/Ir/Pt metallic multilayer nanostructured electrodes, Electrochem. Commun. 13 (2011) 1147.
[11] https://www.nobelprize.org/nobel_prizes/physics/laureates/2007/.
[12] L.A. Kliber, A.M. El-Aziz, R. Hoyer, D.M. Kolb, Tuning reaction rates by lateral strain in a palladium monolayer, Angew. Chem. Int. Ed. 44 (2005) 2080.
[13] T. Bligaard, J.K. Nørskov, Ligand effects in heterogeneous catalysis and electrochemistry, Electrochim. Acta 52 (2007) 5512.
[14] A. Ruban, B. Hammer, P. Stoltze, H.L. Skriver, J.K. Nørskov, Surface electronic structure and reactivity of transition and noble metals, J. Mol. Catal. Chem. 115 (1997) 421.
[15] J.K. Nørskov1, T. Bligaard, J. Rossmeisl, C.H. Christensen, Towards the computational design of solid catalysts, Nat. Chem. 1 (2009) 37.
[16] N. Lopez, T.V.W. Janssens, B.S. Clausen, Y. Xu, M. Mavrikakis, T. Bligaard, J.K. Nørskov, On the origin of the catalytic activity of gold nanoparticles for low-temperature CO oxidation, J. Catal. 223 (2004) 232.
[17] J.K. Nørskov, T. Bligaard, A. Logadottir, S. Bahn, L.B. Hansen, M. Bollinger, H. Bengaard, B. Hammer, Z. Sljivancanin, M. Mavrikakis, Y. Xu, S. Dahl, C.J.H. Jacobsen, Universality in heterogeneous catalysis, J. Catal. 209 (2002) 275.
[18] J. Greeley, J.K. Nørskov, Large-scale, density functional theory-based screening of alloys for hydrogen evolution, Surf. Sci. 601 (2007) 1590.
[19] R. Jinnouchi, K.K.T. Suzuki, Y. Morimoto, DFT calculations on electro-oxidations and dissolutions of Pt and Pt–Au nanoparticles, Catal. Today 262 (2016) 100.
[20] J.R. Kitchin, J.K. Nørskov, M.A. Barteau, J.G. Chen, Modification of the surface electronic and chemical properties of Pt(111) by subsurface 3d transition metals, J. Chem. Phys. 120 (2004) 10240.
[21] J. Greeley, M. Mavrikakis, Competitive paths for methanol decomposition on Pt(111), J. Am. Chem. Soc. 126 (2004) 3910.
[22] F.J. A Broeder, W. Hoving, P.J. H Bloemen, Magnetic anisotropy of multilayers, J. Magn. Magn. Mater. 93 (1991) 562.
[23] L. Smardz, B. Szymanski, R. Gontarz, P. Stefanski, J. Barnas, Interface magnetic anisotropy in metallic superlattices, J. Magn. Magn. Mater. 120 (1993) 239.
[24] K. Spörl, D. Weller, Interface anisotropy and chemistry of magnetic multilayers: Au/Co, Pt/Co and Pd/Co, J. Magn. Magn. Mater. 93 (1991) 379.
[25] P. Gambardella, S. Rusponi, M. Veronese, S.S. Dhesi, C. Grazioli, A. Dallmeyer, I. Cabria, R. Zeller, P.H. Dederichs, K. Kern, C. Carbone, H. Brune, Giant magnetic anisotropy of single cobalt atoms and nanoparticles, Science 300 (2003) 1130.
[26] G. Nabiyouni, Giant magnetoresiscance in spintronic Co/Pt nanowire structures, Metrol. Meas. Syst. 15 (2008) 135.
[27] T. Cren, S. Rusponi, N. Weiss, M. Epple, H. Brune, Oxidation induced enhanced magnetic susceptibility of Co islands on Pt(111), J. Phys. Chem. B 108 (2004) 14685.
[28] L.H. Mendoza-Huizar, J. Robles, M. Palomar-Pardave, Nucleation and growth of cobalt onto different substrates Part I. Underpotential deposition onto a gold electrode, J. Electroanal. Chem. 521 (2002) 95.
[29] L. Cagnon, A. Gundel, T. Devolder, A. Morrone, C. Chappert, J.E. Schmidt, P. Allongue, Anion effect in Co/Au(111) electrodeposition: structure and magnetic behavior, Appl. Surf. Sci. 164 (2000) 22.
[30] V. Georgescu, M. Georgescu, Correlation between microstructure and magnetic properties of electrodeposited Co/Pt multilayers, Surf. Sci. 507 (2002) 507.
[31] S. Schaltin, P. Nockemann, B. Thijs, K. Binnemans, J. Fransaer, Influence of the anion on the electrodeposition of cobalt from imidazolium ionic liquids, Electrochem. Solid state Lett. 10 (2007) D104.
[32] O.E. Kongstein, G.M. Haarberg, J. Thonstad, Current efficiency and kinetics of cobalt electrodeposition in acid chloride solutions. Part I: the influence of current density, pH and temperature, J. Appl. Electrochem. 37 (2007) 669.
[33] E. Lee, S. Kim, J. Jang, H. Park, M.A. Matin, Y. Kim, Y. Kwon, Effects of particle proximity and composition of Pt–M (M= Mn, Fe, Co) nanoparticles on electrocatalysis in methanol oxidation reaction, J. Power Sources 294 (2015) 75.
[34] N.R. Mathe, M.R. Scriba, N.J. Coville, Methanol oxidation reaction activity of microwave-irradiated and heat-treated Pt/Co and Pt/Ni nano-electrocatalysts, Int. Hydrogen Energy 39 (2014) 18871.
[35] R.S. Amin, K.M.E. Khatib, R.M.A. Hameed, E.R. Souaya, M.A. Etman, Synthesis of Pt–Co nanoparticles on multi-walled carbon nanotubes for methanol

oxidation in H_2SO_4 solution, Appl. Catal. Gen. 407 (2011) 195.
[36] R. Ojani, J. Raoof, M. Goli, R. Valiollahi, Pt–Co nanostructures electrodeposited on graphene nanosheets for methanol electrooxidation, J. Power Sources 264 (2014) 76.
[37] R. Nagao, R.G. Freitas, C.D. Silva, H. Varela, E.C. Pereira, Oscillatory electro-oxidation of methanol on nanoarchitectured Pt_{pc}/Rh/Pt metallic multilayer, ACS Catal. 5 (2015) 1045.
[38] A. S. Bondarenko, G. A. Ragoisha. In Progress in Chemometrics Research, Pomerantsev A. L., Ed.; Nova Science Publishers: New York, 2005, pp. 89–102 (the program is available online at: http://www.abc.chemistry.bsu.by/vi/analyser/).
[39] P. Hohenberg, W. Kohn, Inhomogeneous electron gas, Phys. Rev. 136 (1964) B864.
[40] W. Kohn, L.J. Sham, Self-consistent equations including exchange and correlation effects, Phys. Rev. 140 (1965) A1133.
[41] P. Giannozzi, S. Baroni, N. Bonini, M. Calandra, R. Car, C. Cavazzoni, D. Ceresoli, G.L. Chiarotti, M. Cococcioni, I. Dabo, A. DalCorso, S. de Gironcoli, S. Fabris, G. Fratesi, R. Gebauer, U. Gerstmann, C. Gougoussis, A. Kokalj, M. Lazzeri, L. Martin-Samos, N. Marzari, F. Mauri, R. Mazzarello, S. Paolini, A. Pasquarello, L. Paulatto, C. Sbraccia, S. Scandolo, G. Sclauzero, A.P. Seitsonen, A. Smogunov, P. Umari, R.M. Wentzcovitch, Quantum Espresso: a modular and open-source software project for quantum simulations of materials, J. Phys. Condens. Matter 21 (2009) 395502.
[42] A.M. Rappe, K.M. Rabe, E. Kaxiras, J.D. Joannopoulos, Optimized pseudopotentials, Phys. Rev. B 44 (1991) 13175.
[43] J.P. Perdew, K. Burke, M. Ernzerhof, Generalized gradient approximation made simple, Phys. Rev. Lett. 77 (1996) 3865.
[44] H.J. Monkhorst, J.D. Pack, Special points for Brillouin-zone integrations, Phys. Rev. B 13 (1976) 5188.
[45] X. Hong, L. Ehm, Z. Zhong, S. Ghose, T.S. Duffy, D.J. Weidner, High-energy X-ray focusing and applications to pair distribution function investigation of Pt and Au nanoparticles at high pressures, Scient. Rep. 6 (2016) 21434.
[46] A. Kokalj, Computer graphics and graphical user interfaces as tools in simulations of matter at the atomic scale, Comput. Mater. Sci. 28 (2003) 155.
[47] M. Innocenti, F. Loglio, L. Pigani, R. Seeber, F. Terzi, R. Udisti, In situ atomic force microscopy in the study of electrogeneration of polybithiophene on Pt electrode, Electrochim. Acta 50 (2005) 1497.
[48] D.M. Kolb, An atomistic view of electrochemistry, Surf. Sci. 500 (2002) 722.
[49] B.E. Conway, Electrochemical oxide film formation at noble metals as a surface-chemical process, Prog. Surf. Sci. 49 (1995) 331.
[50] S. Trassati, O.A. Petrii, Real surface area measurements in electrochemistry, Pure Appl. Chem. 63 (1991) 719.
[51] R. Baudoing-Savois, P. Dolle, Y. Gauthier, M.C. Saint-Leger, M. De Santis, V. Jahns, Co ultra-thin films on Pt(111) and Co-Pt alloying: a LEED, Auger and synchrotron x-ray diffraction study, J. Phys. Condens. Matter. 11 (1999) 8355.
[52] T. Wadayama, H. Yoshida, K. Ogawa, N. Todoroki, Y. Yamada, K. Miyamoto, Y. Iijima, T. Sugawara, Outermost surface structures and oxygen reduction reaction activities of Co/Pt(111) bimetallic systems fabricated using molecular beam epitaxy, J. Phys. Chem. C 115 (2011) 18589.
[53] M. Shao, K. Sasaki, N.S. Marinkovic, L. Zhang, R.R. Adzic, Synthesis and characterization of platinum monolayer oxygen-reduction electrocatalysts with Co–Pd core–shell nanoparticle supports, Electrochem. Commun. 9 (2007) 2848.
[54] J. Zhang, F.H.B. Lima, M.H. Shao, K. Sasaki, J.X. Wang, J. Hanson, R.R. Adzic, Platinum monolayer on nonnoble Metal–Noble metal Core–Shell nanoparticle electrocatalysts for O_2 reduction, J. Phys. Chem. B 109 (2005) 22701.
[55] http://carine.crystallography.pagespro-orange.fr/.
[56] S. Grazulis, D. Chateigner, R.T. Downs, A.F.T. Yokochi, M. Quiros, L. Lutterotti, E. Manakova, J. Butkus, P. Moeck, A. Le Bail, Crystallography Open Database - an open-access collection of crystal structures, J. Appl. Crystallogr. 42 (2009) 726.
[57] F. Maillard, E.R. Savinova, P.A. Simonov, V.I. Zaikovskii, U. Stimming, Infrared spectroscopic study of CO adsorption and electro-oxidation on carbon-supported Pt Nanoparticles: interparticle versus intraparticle heterogeneity, J. Phys. Chem. B 108 (2004) 17893.
[58] R.M. Arán-Ais, F.J. Vidal-Iglesias, M.J.S. Farias, J. Solla-Gullón, V. Montiel, E. Herrero, J.M. Feliu, Understanding CO oxidation reaction on platinum nanoparticles, J. Electroanal. Chem. 793 (2017) 126.
[59] J.S. Spendelow, G.Q. Lu, P.J.A. Kenis, A. Wieckowski, Electrooxidation of adsorbed CO on Pt(111) and Pt(111)/Ru in alkaline media and comparison with results from acidic media, J. Electroanal. Chem. 568 (2004) 215.
[60] H. Zhao, J. Yang, L. Li, H. Li, J. Wang, Y. Zhang, Effect of over-oxidation treatment of Pt–Co/polypyrrole-carbon nanotube catalysts on methanol oxidation, Int. J. Hydrogen Energy 34 (2009) 3908.
[61] M. Wakisaka, S. Mitsui, Y. Hirose, K. Kawashima, H. Uchida, M. Watanabe, Electronic structures of Pt–Co and Pt–Ru alloys for CO-tolerant anode catalysts in polymer electrolyte fuel cells studied by EC–XPS, J. Phys. Chem. B 110 (2006) 23489.
[62] M. P. Hyman, J. W. Medlin, Effects of electronic structure modifications on the adsorption of oxygen reduction reaction intermediates on model Pt(111)-Alloy surfaces, J. Phys. Chem. C 111 (2207) 17052.
[63] T. Iwasita, Electrocatalysis of methanol oxidation, Electrochim. Acta 47 (2002) 3663.
[64] B. Beden, F. Kardigan, C. Lamy, J.M. Leger, Electrocatalytic oxidation of methanol on platinum-based binary electrodes, J. Electroanal. Chem. 127 (1981) 75.
[65] H.A. Gasteiger, N. Markovic, P.N. Ross, E.J. Cairns, Temperature-dependent methanol electro-oxidation on well-characterized Pt-Ru alloys, J. Electrochem. Soc. 141 (1994) 1795.
[66] T. Zerihun, P. Grundler, Oxidation of formaldehyde, methanol, formic acid and glucose at ac heated cylindrical Pt microelectrodes, J. Electroanal. Chem. 441 (1998) 57.
[67] R.S. Amin, K.M.E. Khatib, R.M.A. Hameed, E.R. Souaya, M.A. Etman, Synthesis of Pt–Co nanoparticles on multi-walled carbon nanotubes for methanol oxidation in H_2SO_4 solution, Appl. Catal. Gen. 407 (2011) 195.
[68] E. Antolini, J.R.C. Salgado, E.R. Gonzalez, The methanol oxidation reaction on platinum alloys with the first row transition metals: the case of Pt–Co and–Ni alloy electrocatalysts for DMFCs: a short review, Appl. Catal. B Environ. 63 (2006) 137.
[69] J.T. Muller, P.M. Urban, W.F. Holderich, J. Power Sources 84 (1999) 157.
[70] D.A. Harrington, B.E. Conway, Ac Impedance of Faradaic reactions involving electrosorbed intermediates—I. Kinetic theory, Electrochim. Acta 32 (1987) 1703.
[71] F. Seland, R. Tunold, D.A. Harrington, Impedance study of formic acid oxidation on platinum electrodes, Electrochim. Acta 53 (2008) 6851.
[72] E. Budevski, G. Staikov, W. J. Lorenz in Electrochemical Phase Growth VCH New York-USA (1996) Chap. 01 pg. 06.
[73] J.S. Tsay, Y.E. Wu, C.S. Shen, Growth mode and inter-diffusion of Co on Pt(111), Chin. J. Phys. 35 (1997) 610.
[74] P.C. McIntyre, D.T. Wu, M. Natsasi, Interdiffusion in epitaxial Co/Pt multilayers, J. Appl. Phys. 81 (1997) 637.
[75] P. Piela, R. Fields, P. Zelenay, Electrochemical impedance spectroscopy for direct methanol fuel cell diagnostics, J. Electrochem. Soc. 153 (2006) 1902.
[76] V.S. Bagotzky, Y.B. Vassilyev, Mechanism of electro-oxidation of methanol on the platinum electrode, Electrochim. Acta 12 (1967) 1323.
[77] L. Chen, M. Guo, H.F. Zhan, X.D. Wang, Characterization and electrocatalytic properties of PtRu/C catalysts prepared by impregnation-reduction method using Nd_2O_3 as dispersing reagent, Electrochim. Acta 52 (2006) 1191.
[78] M.W. Finnis, The energy and elastic constants of simple metals in terms of pairwise interactions, J. Phys. F Met. Phys. 4 (1974) 1645.
[79] A. Michaelides, M. Scheffler, Surface and interface science, Volume vol. 1: Concepts and Methods, Editor Klaus Wandelt Ed. Wiley-VCH (2012) ISBN: 978-3-527-41156-6.
[80] R. Smoluchowski, Anisotropy of the electronic work function of metals, Phys. Rev. 60 (1941) 661.